PERGAMON

International Journal of Solids and Structures 36 (1999) 3677–3708

INTERNATIONAL JOURNAL OF SOLIDS and STRUCTURES

On the minimum weights of compression structures

Bernard Budiansky*

Division of Engineering and Applied Sciences, Harvard University, Pierce Hall 313, Cambridge, MA 02138, U.S.A.

Received 21 January 1998; in revised form 21 May 1998

Abstract

The weights of optimal compression structures of several types are estimated. Minimum weights of columns having solid square or circular cross-sections are compared with those of similar metal–foam-filled tubes, hollow tubes and tubes whose walls are foam-core sandwiches. Similarly, the minimum (of near-minimum) weights of wide sandwich compression panels are studied along with those of hat-stiffened, solid-skin panels and panels in which the skins and stiffeners are themselves metal–foam-core sandwiches. In these studies, weight comparisons are made on the basis of appropriate structural indices and compressive strength is the only failure criterion. These studies provide baseline comparisons that ignore other possible design constraints, such as longitudinal stiffness, minimum gage and cost.

1. Introduction

For many years, light-core sandwich construction has been considered as an alternative to conventional thin-gage compression structures, such as skin-stringer panels. Recent advances in the processing of metallic foams having porosities as high as 0.95 has aroused interest in their potential use as structural sandwich cores. Accordingly, the purpose of the present paper is to make some elementary baseline efficiency studies that explore how well metal–foam-core compression structures might compete purely on the basis of the minimum structural weight needed to carry prescribed loads over given distances. Compressive strength is the only design constraint imposed in the present studies and the approach used exploits classical concepts of structural index and minimum-weight design that were established, applied and extended by Wagner (1929), Zahorski (1944), Schuette (1945), Farrar (1949), Shanley (1952), Gerard (1956) and more recently and extensively, by Weaver and Ashby (1997). Factors other than strength that might be pertinent to the design process, such as cost, longitudinal stiffness, or minimum gage, are not considered here.

Several kinds of configurations have been selected for comparative minimum-weight analysis.

* E-mail: budiansky@husm.harvard.edu

0020–7683/99/$ - see front matter
PII: S0020–7683(98)00169–3

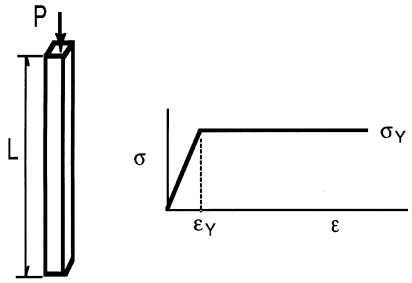

Fig. 1. Column load and length; stress–strain relation.

Columns having solid square or circular cross-sections are compared with similar foam-filled tubes, with hollow tubes and tubes whose walls are foam-core sandwiches. Similarly, the weights of optimized (or near-optimum) skin-stringer panels are studied together with those of minimum-weight sandwich panels and those of skin-stringer panels in which skins and stiffeners are themselves metal–foam-core sandwiches. In each optimization study, the porosity of the metal foam is held fixed (that is, optimization with respect to porosity is not executed) and the various general conclusions drawn are limited to porosities around 90–95%.

The present study is not, of course, a substitute for the elaborate computation-intensive industrial procedures for structural analysis, design and optimization that have come into use in recent decades. In all of the present calculations, geometries are idealized (for example, details of riveted attachments are ignored) and various approximations are introduced that facilitate the analyses without doing violence to the broad general conclusions reached.

2. Columns

2.1. Ideal plasticity

Much of the analysis here elaborates on the work of Gerard (1956). With the strength P and length L of a simply-supported column prescribed (Fig. 1), the minimum weights of untapered columns of various types, with and without the incorporation of lightweight foam material, will be calculated and compared. The base material has Young's modulus E and weight density ρ and is elastic–ideally plastic, with compressive stress σ and strain ε related by $\sigma = E\varepsilon$ for σ less than the yield stress σ_Y and $\sigma = \sigma_Y$ for $\varepsilon > \varepsilon_Y = \sigma_Y/E$.

2.2. Homogeneous columns; structural index; stress bounds

In a homogeneous column (i.e., no foam) having any cross-sectional shape, the axial stress σ produced by the design load P must satisfy the inequality

$$\sigma \leqslant \sigma_1 \equiv \frac{\pi^2 EI}{AL^2} \tag{1}$$

where A is the cross-sectional area, I is its minimum moment of inertia and σ_1 is the Euler column buckling stress. This is the same as

$$\sigma \leqslant \frac{\pi^2 \beta E A}{L^2} \tag{2}$$

where β is the non-dimensional shape factor $\beta = I/A^2$. Substituting $A = P/\sigma$ gives

$$\sigma \leqslant \pi \sqrt{E\beta} \sqrt{\frac{P}{L^2}} \tag{3}$$

in terms of the structural index P/L^2 (Wagner, 1929), which captures the prescribed design variables P and L. But σ can also not exceed the yield stress σ_Y and so, in the minimum-weight analyses that follow, the stress bounds

$$\frac{\sigma}{E} \leqslant \frac{\pi^2 I}{AL^2} \equiv \frac{\sigma_1}{E} \tag{4a}$$

or

$$\frac{\sigma}{E} \leqslant \pi \sqrt{\beta} \left(\frac{P}{EL^2} \right)^{1/2} \tag{4b}$$

and

$$\frac{\sigma}{E} \leqslant \varepsilon_Y \tag{5}$$

must be satisfied for each prescribed value of the nondimensional structural index $P/(EL^2)$. The weight of the column is $W = \rho A L$ and again using $A = P/\sigma$ gives the equation

$$\frac{W}{\rho L^3} = \frac{\dfrac{P}{EL^2}}{\sigma/E} \tag{6}$$

for the non-dimensional weight $W/(\rho L^3)$. Thus, in a homogeneous column, maximising the stress minimizes the weight. If local buckling is an issue, stress constraints in addition to (4), (5) generally have to be imposed.

2.3. *Compact, homogeneous cross-sections: circles and squares*

For a solid circular cross-section, $\beta = (4\pi)^{-1}$ and minimum weight is obtained by substituting into eqn (6) the largest allowable stress permitted by one or the other of the constraints (4b) and (5). This gives (Gerard, 1956)

$$\frac{W_{\min}}{\rho L^3} = \frac{2}{\sqrt{\pi}} \left(\frac{P}{EL^2} \right)^{1/2} \quad \text{for } \frac{P}{EL^2} \leqslant \frac{4\varepsilon_Y^2}{\pi}$$

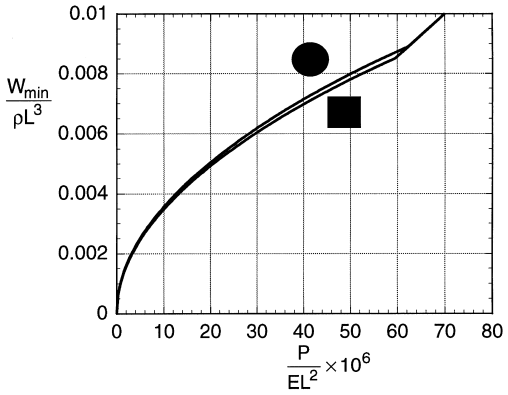

Fig. 2. Minimum column weights for solid circular and square cross-sections, $\varepsilon_Y = 0.007$.

$$= \frac{P}{\varepsilon_Y EL^2} \quad \text{for} \frac{P}{EL^2} \geqslant \frac{4\varepsilon_Y^2}{\pi}. \tag{7}$$

A similar calculation for a column having a solid square cross-section, with $\beta = 1/12$, gives

$$\frac{W_{\min}}{\rho L^3} = \frac{2\sqrt{3}}{\pi}\left(\frac{P}{EL^2}\right)^{1/2} \quad \text{for} \frac{P}{EL^2} \leqslant \frac{12\varepsilon_Y^2}{\pi^2}$$

$$= \frac{P}{\varepsilon_Y EL^2} \quad \text{for} \frac{P}{EL^2} \geqslant \frac{12\varepsilon_Y^2}{\pi^2}. \tag{8}$$

These results are plotted in Fig. 2 for the choice $\varepsilon_Y = 0.007$. The square is slightly more efficient than the circle, up to the value of the structural index at which they both fail at the 'squash' load $\sigma_Y A$. Note that for all cross-sections, $W_{\min}/(\rho L^3) = P/(\varepsilon_Y EL^2)$ provides a universal lower bound on the weight and so represents the highest conceivable structural efficiency at any value of the structural index.

2.4. Foam-core columns

Consider next a foam-filled column having the square cross-section show in Fig. 3, with the weight density of the foam core equal to $\rho_c < \rho$. The following simplifying assumptions will be made in the minimum weight analysis that follows:

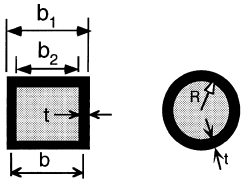

Fig. 3. Foam-core tubes. Square: $t = (b_1 - b_2)/2$, $b = (b_1 + b_2)/2$; circle: R = mean radius.

- the core stabilizes the tube walls against local buckling;
- the contribution of the core to the column bending stiffness is neglected;
- the contribution of the compressive stress in the core to the total applied load is neglected;
- reduction of the column buckling strength due to transverse shear compliance is neglected.

Accordingly, with $A = b_1^2 - b_2^2$, $I = (b_1^4 - b_2^4)/12$ and $\sigma = P/A$, the constraint eqns (4), (5) continue to apply, with

$$\frac{\sigma_1}{E} = \frac{\pi^2}{12}\left(\frac{b_1^2 + b_2^2}{L^2}\right). \tag{9}$$

The total weight $W = \rho AL + \rho_c b_2^2 L$ is $W = (\rho - \rho_c/2)AL + \rho_c(b_1^2 + b_2^2)L/2$ and using $A = P/\sigma$ as well as eqn (9) leads to the non-dimensional weight equation

$$\frac{W}{\rho L^3} = \frac{\left(1 - \dfrac{\rho_c}{2\rho}\right)\dfrac{P}{EL^2}}{\sigma/E} + \frac{6}{\pi^2}\frac{\rho_c}{\rho}\frac{\sigma_1}{E}. \tag{10}$$

For minimum weight, we want the lowest possible σ_1 consistent with the constraint (4a); this implies that σ_1 should be set equal to σ in (10), as long as the constraint (5) is not violated. Then minimization of (10) with respect to σ/E leads to

$$\frac{\sigma_1}{E} = \frac{\sigma}{E} = \pi\sqrt{\left(\frac{\rho}{6\rho_c}\right)\left(1 - \frac{\rho_c}{2\rho}\right)\left(\frac{P}{EL^2}\right)} \tag{11}$$

and

$$\frac{W_{\min}}{\rho L^3} = \frac{2}{\pi}\sqrt{\left(\frac{6\rho_c}{\rho}\right)\left(1 - \frac{\rho_c}{2\rho}\right)\left(\frac{P}{EL^2}\right)} \tag{12}$$

for $P/(EL^2) \leqslant [P/(EL^2)]_Y$, where

$$\left(\frac{P}{EL^2}\right)_Y = \frac{6}{\pi^2}\frac{\rho_c}{\rho}\left(1 - \frac{\rho_c}{2\rho}\right)^{-1}\varepsilon_Y^2 \tag{13}$$

is the critical value of the structural index for which the stress σ in (11) becomes equal to σ_Y. For higher values of $P/(EL^2)$, minimum weight is associated with the attainment of both of the upper bounds on σ in eqns (4a) and (5) and so we can set $\sigma_1/E = \sigma/E = \varepsilon_Y$ in (10) to get

$$\frac{W_{\min}}{\rho L^3} = \frac{\left(1 - \dfrac{\rho_c}{2\rho}\right)\dfrac{P}{EL^2}}{\varepsilon_Y} + \frac{6}{\pi^2}\frac{\rho_c}{\rho}\varepsilon_Y \tag{14}$$

in the range $[P/(EL^2)]_Y \leqslant P/(EL^2) \leqslant [P/(EL^2)]_S$. Here

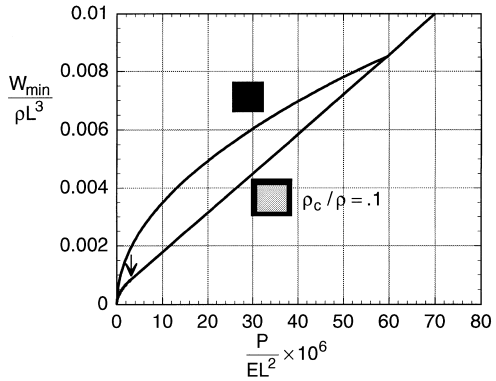

Fig. 4. Minimum weights of solid and foam-core columns, $\varepsilon_Y = 0.007$, $\rho_c/\rho = 0.1$. The arrow indicates $[P/(EL^2)]_Y$ and the curves meet at $[P/(EL^2)]_S$; see eqns (13), (15).

$$\left(\frac{P}{EL^2}\right)_S = \frac{12\varepsilon_Y^2}{\pi^2} \tag{15}$$

is the same breakpoint discovered in eqn (8) for the transition to squashing failure of the optimum column of solid square cross-section. This means that for all higher values of $P/(EL^2)$, the foam-core column is solid, the optimum amount of foam having become zero; the buckling constraint becomes irrelevant, the optimum column fails at its squash load and we have $W_{min}/(\rho L^3) = P/(\varepsilon_Y EL^2)$. These results for minimum weight are plotted in Fig. 4, for $\rho_c/\rho = 0.1$ and $\varepsilon_Y = 0.007$, together with those for the solid square. Clearly, over a substantial range of structural index, the optimum foam-core column weighs considerably less that the solid column—not a surprise.

For $P/(EL^2) \leqslant [P/(EL^2)]$ the optimum dimensions of the foam-core column are determined by the relations (9) and

$$\frac{\sigma}{E} = \frac{P}{AE} = \frac{P/(EL^2)}{(b_1^2 - b_2^2)/L^2}. \tag{16}$$

Solving for b_1 and b_2 gives

$$\frac{b_{1,2}}{L} = \frac{1}{\sqrt{2}}\left\{\frac{12}{\pi^2}\frac{\sigma_1}{E} \pm \frac{P/(EL^2)}{\sigma/E}\right\}^{1/2}. \tag{17}$$

Sample plots are shown in Fig. 5. Here, for $P/(EL^2) \leqslant [P/(EL^2)]_Y$, the result (11) for $\sigma/E = \sigma_1/E$ is used in eqn (17), while for $[P/(EL^2)]_Y \leqslant P/(EL^2) \leqslant [P/(EL^2)]_S$, $\sigma/E = \sigma_1/E = \varepsilon_Y$. For $P/(EL^2) \geqslant [P/(EL^2)]_S$, we have $\sigma/E = \varepsilon_Y$ and $b_2 = 0$ and then eqn (16) gives $b_1/L = [P/(\varepsilon_Y EL^2)]^{1/2}$.

In the elastic design range, for $P/(EL^2) \leqslant [P/(EL^2)]_Y$, the optimum ratio of core weight to skin weight is exactly

$$\frac{W_c}{W_s} = 1 - \frac{\rho_c}{\rho} \tag{18}$$

and in this initial range the ratio t/b (see Fig. 3) is very nearly constant at

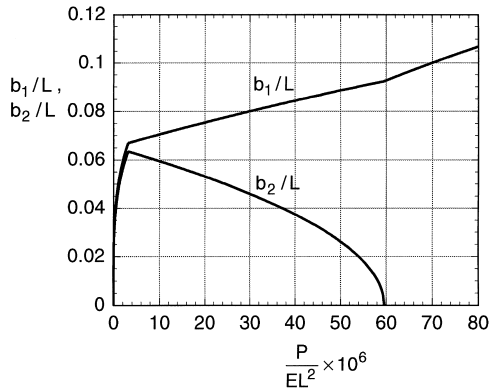

Fig. 5. Optimum dimension ratios of foam-core column, $\varepsilon_Y = 0.007$, $\rho_c/\rho = 0.1$; Fig. 3.

$$\frac{t}{b} = \frac{\rho_c}{4\rho}\left(1-\frac{\rho_c}{2\rho}\right)^{-1}. \tag{19}$$

A very similar analysis for a foam-core circular-cylinder column gives the following results for minimum weight:

$$\begin{aligned}\frac{W_{\min}}{\rho L^3} &= 2\sqrt{\left(\frac{2\rho_c}{\pi\rho}\right)\left(1-\frac{\rho_c}{2\rho}\right)\left(\frac{P}{EL^2}\right)} \quad \text{for } \frac{P}{EL^2} \leqslant \frac{2\rho_c}{\pi\rho}\left(1-\frac{\rho_c}{2\rho}\right)^{-1}\varepsilon_Y^2 \\ &= \left(1-\frac{\rho_c}{2\rho}\right)\frac{P}{\varepsilon_Y EL^2} + \frac{2\rho_c}{\pi\rho}\varepsilon_Y \quad \text{for} \frac{2\rho_c}{\pi\rho}\left(1-\frac{\rho_c}{2\rho}\right)^{-1}\varepsilon_Y^2 \leqslant \frac{P}{EL^2} \leqslant \frac{4\varepsilon_Y^2}{\pi} \\ &= \frac{P}{\varepsilon_Y EL^2} \quad \text{for } \frac{P}{EL^2} \geqslant \frac{4\varepsilon_Y^2}{\pi}.\end{aligned} \tag{20}$$

The relation (18) for W_c/W_s also holds here in the initial, elastic range, wherein t/R (see Fig. 3.) remains very close to

$$\frac{t}{R} = \frac{\rho_c}{2\rho}\left(1-\frac{\rho_c}{2\rho}\right)^{-1}. \tag{21}$$

The optimum weights (20) for the foam-filled circular cylinder are just a few percent higher than those for the foam-filled square tube, until they become equal to each other when both optimum columns have become solid and fail by squashing, for $P/(EL^2) > 4\varepsilon_Y^2/\pi$.

2.5. *Hollow square tubes*; *naive optimization*; *mode interaction*

The optimization analysis by Gerard (1956) of a hollow square tube (Fig. 3, with the foam core removed) will now be recapitulated. Recall [eqn (6)] that for minimum weight, the allowable stress

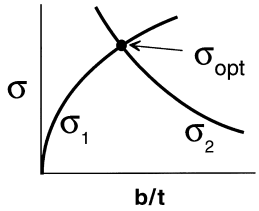

Fig. 6. Optimum stress for given structural index $P/(EL^2)$; σ_1 = Euler buckling constraint, σ_2 = local plate buckling constraint.

should be maximized at the optimum design. For t/b small, $\beta \approx (1/24)(b/t)$ in the Euler buckling constraint (4b) and so

$$\frac{\sigma}{E} \leqslant \frac{\pi}{\sqrt{24}} \left(\frac{P}{EL^2}\right)^{1/2} \sqrt{\frac{b}{t}} \equiv \frac{\sigma_1}{E}. \tag{22}$$

For a prescribed value of the structural index, the upper bound σ_1 on σ is an increasing function of b/t (Fig. 6). But the stress σ must also satisfy the constraint

$$\sigma \leqslant \sigma_2 \equiv \frac{4\pi^2 D}{b^2 t} \tag{23}$$

where σ_2 is the local plate buckling stress and

$$D = \frac{Et^3}{12(1-\nu^2)} \tag{24}$$

is the plate bending stiffness. (Here we assume a pattern of simply-supported square buckles around and along the tube, which is a good approximation for $L \gg b$.) Hence

$$\frac{\sigma}{E} \leqslant \frac{\pi^2}{3(1-\nu^2)} \left(\frac{t}{b}\right)^2 = \frac{\sigma_2}{E} \tag{25}$$

and here σ_2 is a decreasing function of b/t. Accordingly, in the absence of plastic yielding, the optimum choice of b/t, namely, the one that maximizes σ under the simultaneous constraints (22) and (25), makes $\sigma_1 = \sigma_2 = \sigma_{\text{opt}}$ (Fig. 6). This condition implies

$$\frac{\sigma_{\text{opt}}}{E} = (1-\nu^2)^{-1/5} \left(\frac{\pi^2}{12}\right)^{3/5} \left(\frac{P}{EL^2}\right)^{2/5} \tag{26}$$

(Gerard, 1956) and the corresponding minimum weight $W_{\min}$ that follows from eqn (6) satisfies

$$\frac{W_{\min}}{\rho L^3} = (1-\nu^2)^{1/5} \left(\frac{12}{\pi^2}\right)^{3/5} \left(\frac{P}{EL^2}\right)^{3/5}. \tag{27}$$

From (25), the optimum value of t/b is

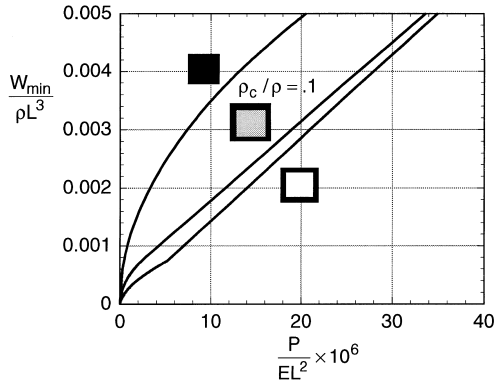

Fig. 7. Minimum weights of solid, foam-core and hollow square cross-section columns; $\varepsilon_Y = 0.007$, $\nu = 1/3$.

$$\frac{t}{b} = \frac{\sqrt{3(1-\nu^2)}}{\pi}\sqrt{\frac{\sigma_{opt}}{E}} \tag{28}$$

and with $I/A \approx b^2/6$, eqn (4a) gives

$$\frac{b}{L} = \frac{\sqrt{6}}{\pi}\sqrt{\frac{\sigma_{opt}}{E}}. \tag{29}$$

The results in eqns (26)–(29) do not, of course, apply if the value of σ_{opt}/E given by eqn (26) exceeds the yield condition (5). This will happen for

$$\frac{P}{EL^2} > (1-\nu^2)^{1/2}\left(\frac{12}{\pi^2}\right)^{3/2}\varepsilon_Y^{5/2} \tag{30}$$

and then the familiar result $(W_{min}/\rho L^3) = (P/EL^2\varepsilon_Y)$ corresponding to squashing failure holds.

For $\varepsilon_Y = 0.007$, the hollow-tube minimum weight is compared in Fig. 7 with the optimum weights of solid and foam-core columns. The optimized hollow tube evidently weighs less than the best tubes filled with 90%-porosity metal foam. It is noteworthy that for the hollow tube, the result for minimum weight [eqn (27)] in the elastic range varies like the 3/5th power of the structural index, while for foam-filled columns the weight given by eqn (18) is proportional to the square root of the index. This means that if plasticity did not occur the foam-filled tube would eventually become more efficient at a sufficiently high value of the structural index. However, for practical values of ε_Y, plasticity does intervene and the hollow tube stays lighter. The weight margin is, of course, reduced for lower foam-core density.

The optimum dimension ratios (28), (29) for the hollow tube are exhibited in Fig. 8, up to the squashing transition value (30) of the structural index. In the plastic design range, for which $P = 4bt\sigma_Y$, the constraint

$$4\left(\frac{t}{b}\right)\left(\frac{b}{L}\right)^2\varepsilon_Y = \frac{P}{EL^2} \tag{31}$$

must apply. Also, to ensure that elastic buckling does not occur, the inequalities

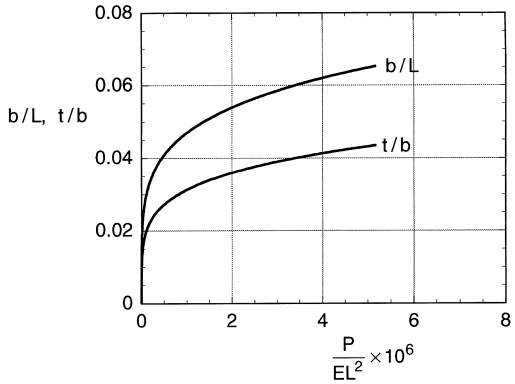

Fig. 8. Optimum dimension ratios (Fig. 3) for hollow square-tube column; $\varepsilon_Y = 0.007$, $\nu = 1/3$.

$$\frac{t}{b} \geqslant \frac{\sqrt{3(1-\nu^2)\varepsilon_Y}}{\pi}, \quad \frac{b}{L} \geqslant \frac{\sqrt{6\varepsilon_Y}}{\pi} \tag{32}$$

implied by eqns (25), (4a) must hold. But the relations (31), (32) do not determine unique optimum values for t/b and b/L; minimum weights are obtained for a range of designs in the plastic range.

The optimum design procedure used in the elastic range, in which two independent modes of failure were forced to occur simultaneously, has been called 'naive optimization' (Maquoi and Massonet, 1976). Why 'naive'? The simple-minded concept is that if there is a residual margin of safety with respect to secondary failure mode when primary failure occurs, the structure has been over-designed.[1] But even when this approach appears to be rigorous, as in the derivation just shown, the failure modes may not really be independent in the presence of small geometrical imperfections and they may be susceptible to a strong non-liner interaction. On this basis, many warnings have been issued against naive optimization (e.g., Koiter and Skaloud, 1962; Thompson and Lewis, 1972; Tvergaard, 1973); optimizing configurations may not be correctly predicted and more seriously, strength may be degraded because of multi-mode imperfection-sensitivity in the vicinity of optimum configurations. These mode-interaction issues are encapsulated in the schematic diagrams shown in Fig. 9. Here the thick lines in the first two sketches illustrate elastic buckling and initial postbuckling load–displacement relations for imperfection-free columns and plates. In naive optimization of the perfect hollow, square-tube column, these buckling loads P_c coincide and the last drawing shows the load deflection behavior when the two buckling modes interact non-linearly. Although the uncoupled buckling behaviors are stable, the combined behavior displays a falling post-buckling load. In the presence of initial geometrical imperfections, the uncoupled and coupled load-deflection behaviors are illustrated by the thin lines and the salient point to be made is that mode interaction leads to an actual buckling strength that is reached at

[1] This is the principle of the poem "The Deacon's Masterpiece; or The Wonderful 'One-Hoss Shay'" by Oliver Wendell Holmes, in which every part of the parson's horse-drawn chaise was just as strong as every other part; so that when it finally failed after a century of use, "it went to pieces all at once... and nothing first". The poem concludes: "Logic is logic. That's all I say."

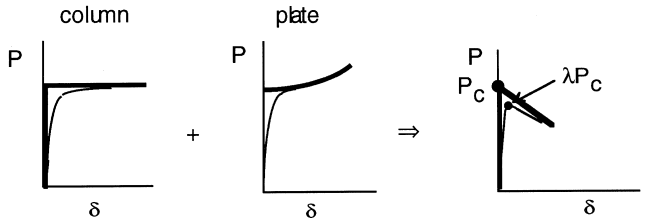

Fig. 9. Nonlinear interaction of column and plate buckling modes.

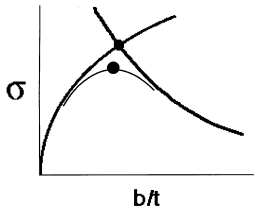

Fig. 10. Actual and naive design optima.

the limit point λP_c, where $\lambda < 1$ is a knockdown factor that depends on the sizes and shapes of the imperfections. This phenomenology was exposed in the classic work by Koiter (1945) and in the many later warnings against naive optimization. The mode interaction might be accentuated in structures for which one or more of the individual buckling modes are themselves unstable.

An additional consequence of mode interaction is suggested in Fig. 10, which reproduces the diagram of Fig. 6 showing the naive-optimum dimension ratio b/t, together with the optimum design point on the thin line for the actual relation between the strength and b/t. Although there can be exceptions (e.g., Thompson and Lewis, 1972) the smooth maximum on this relation is generally not far from the b/t dictated by naive optimization. Studies by Koiter and his co-workers (e.g., Koiter and Pignataro, 1976) suggest that the earlier warnings were generally too severe and that a value of $\lambda \approx 0.9$ should often be conservative in mode-interaction situations. But λ could sometimes be smaller; definitive, generalized conclusions are hard to glean from the literature.

So, to take mode-interaction into account approximately in an optimization calculation when a load P is specified, a plausible approach is to execute naive optimization for an amplified magnitude P/λ for the specified load. If λ really is the knockdown factor, the resulting structure would have the right strength and be close to optimum. Thus, the minimum-weight results for the hollow tube in Fig. 7 can be reinterpreted by defining the abscissa to be $P/(\lambda EL^2)$. The results found for optimum dimension ratios may similarly be redefined to be functions of $P/(\lambda EL^2)$. Since there is no mode interaction in the solid or foam-filled tubes, we would keep $\lambda = 1$ for these cases. If we choose $\lambda = 0.9$ for the hollow tube, Fig. 7 still indicates that it has the lowest weight for a given value of $P/(EL^2)$. Whether we should continue to use this modest knockdown factor in the squashing range of the hollow tube is problematic; it might be somewhat lower in the vicinity of $P/(EL^2) \times 10^6 = 5$. Even there, for $\rho_c/\rho = 0.1$ and λ as low as 0.5, the foam-filled square tube would still not be preferable the hollow tube on the basis of weight.

2.6. Hollow circular tubes

Gerard (1956) also studied the optimum hollow circular cylinder, for which some new issues arise; his treatment is revised slightly here. For small t/R (Fig. 3) the column buckling stress is

$$\sigma_1 = \frac{\pi^2 E}{2}\left(\frac{R}{L}\right)^2. \tag{33}$$

The local shell buckling stress will be written as

$$\sigma_2 = \gamma \frac{E}{\sqrt{3(1-\nu^2)}}\frac{t}{R} \tag{34}$$

where γ is a knockdown factor that multiplies the classical critical stress for a perfect cylinder. The local buckling of a circular cylinder is notoriously imperfection-sensitive and γ takes this into account before any additional knockdown is introduced by coupling with the column buckling mode. The empirical choice made here for γ as a function of t/R is that suggested by NASA (Anon., 1965), namely

$$\gamma = 1 - 0.901(1 - \mathrm{e}^{-\phi}) \tag{35}$$

where

$$\phi = \frac{1}{16}\sqrt{\frac{R}{t}}. \tag{36}$$

This dependence of γ on t/R is based on a lower bound to reams of critical-stress data on cylindrical shell buckling. Setting $\sigma_1 = \sigma_2 = \sigma$ in accordance with the naive optimization criterion and using

$$\frac{P}{EL^2} = 2\pi\left(\frac{R}{L}\right)^2\left(\frac{t}{R}\right)\frac{\sigma}{E} \tag{37}$$

together with eqns (33), (34) and eqn (6) permits the explicit evaluation of σ/E, R/L, $P/(EL^2)$ and finally $W_{\min}/(\rho L^3)$ in terms of t/R. Squash-load design takes over [eqn (5)] for

$$\gamma t/R \geqslant \varepsilon_Y\sqrt{3(1-\nu^2)}. \tag{38}$$

(For $\varepsilon_Y = 0.007$ and $\nu = 1/3$, this starts at $(t/R)_S \approx 0.0173$, where $\gamma = 0.659$.) The final step is to introduce the mode-interaction factor λ and plot results against $P/(\lambda EL^2)$ instead of $P/(EL^2)$. This is done in Fig. 11, where the hollow circular tube weights are compared with those for the foam-core and hollow squares. (Assign $\lambda = 1$ for the foam-core column weight, whereas $\lambda < 1$ for the other two curves.) The optimum hollow circle squashes at $P/(\lambda EL^2)_S = 1.08 \times 10^{-6}$ and provides the lowest weight up to the squash transition value $P/(\lambda EL^2)_S = 5.18 \times 10^{-6}$ for the hollow square. In this assessment, it is presumed that λ is about the same, say 0.9, for the hollow square and hollow circle, although information for the latter is lacking. Plots showing the optimum dimension ratios t/R and R/L, omitted here, may be easily generated; as for the hollow square tube, optimum proportions are not unique in the squashing domain.

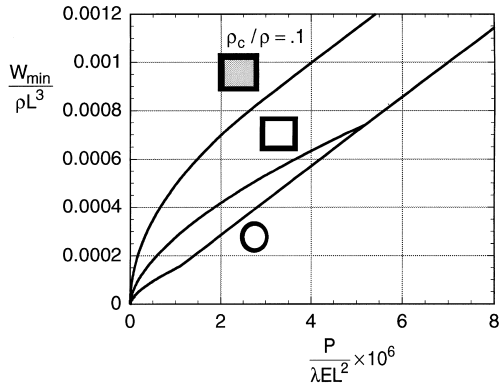

Fig. 11. Comparison of minimum weights for hollow circular cylinder, foam-core square and hollow square; $\varepsilon_Y = 0.007$, $v = 1/3$.

2.7. Hollow square tubes with sandwich walls

Consider next a hollow-core column of square cross-section, the walls of which are themselves sandwiches (Fig. 12). Each sandwich face sheet has thickness t; the face-sheet spacing, measured between sheet midplanes, is $d \geqslant t$; the centerline width of the square is b. The column buckling stress σ_1 remains well approximated by eqn (4a) with $I/A \approx b^2/6$. The plate bending stiffness of the sandwich walls is

$$D = \frac{E}{1-v^2}\left(\frac{td^2}{2}\right)\left[1+\frac{1}{3}\left(\frac{t}{d}\right)^2\right] \tag{39}$$

and so the local plate buckling stress is

$$\sigma_2 = \frac{4\pi^2 D}{2b^2 t} = \frac{\pi^2 E}{1-v^2}\left(\frac{d}{b}\right)^2\left[1+\frac{1}{3}\left(\frac{t}{d}\right)^2\right]. \tag{40}$$

Invoking the naive optimization condition $\sigma_1 = \sigma_2 = \sigma$ provides the connections

$$\frac{\sigma}{E} = \frac{\pi^2}{6}\left(\frac{b}{L}\right)^2 = \frac{\pi^2}{1-v^2}\left(\frac{d}{b}\right)^2\left[1+\frac{1}{3}\left(\frac{t}{d}\right)^2\right] \tag{41}$$

for optimum design in the elastic range. The weight of the column is

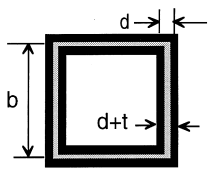

Fig. 12. Cross-section of hollow, square-tube column with sandwich walls.

$$W = [8\rho bt + 4\rho_c b(d-t)]L \tag{42}$$

and we can use the exact relation

$$P = 8\sigma bt \tag{43}$$

to eliminate t and get

$$\frac{W}{\rho L^3} = \frac{\left(1-\frac{1}{2}\frac{\rho_c}{\rho}\right)\frac{P}{EL^2}}{\sigma/E} + \frac{4\rho_c}{\rho}\left(\frac{b}{L}\right)^2\frac{d}{b}. \tag{44}$$

Now eliminate b/L and d/b in favor of σ via eqns (41), dropping for the nonce the term $\frac{1}{3}(t/d)^2$, which will turn out to be entirely negligible in the elastic design range. This gives

$$\frac{W}{\rho L^3} = \frac{\left(1-\frac{1}{2}\frac{\rho_c}{\rho}\right)\frac{P}{EL^2}}{\sigma/E} + \frac{24\sqrt{(1-\nu^2)}}{\pi^3}\frac{\rho_c}{\rho}(\sigma/E)^{3/2} \tag{45}$$

which, finally, may be minimized analytically with respect to σ/E to get $W_{\min}$. The results are

$$\frac{\sigma_{opt}}{E} = [1-\nu^2]^{-1/5}\left[\frac{\pi^3/36}{\rho_c/\rho}\left(1-\frac{1}{2}\frac{\rho_c}{\rho}\right)\right]^{2/5}\left[\frac{P}{EL^2}\right]^{2/5} \tag{46}$$

and

$$\frac{W}{\rho L^3} = \frac{10}{\pi}\left(\frac{1-\nu^2}{6\pi}\right)^{1/5}\left(\frac{\rho_c}{\rho}\right)^{2/5}\left(1-\frac{1}{2}\frac{\rho_c}{\rho}\right)^{3/5}\left(\frac{P}{EL^2}\right)^{3/5}. \tag{47}$$

From (41), the corresponding optimum values of b/L and d/b are

$$\frac{b}{L} = \frac{\sqrt{6}}{\pi}\sqrt{\frac{\sigma_{opt}}{E}}, \quad \frac{d}{b} = \frac{1}{\pi}\sqrt{\frac{(1-\nu^2)\sigma_{opt}}{E}} \tag{48}$$

with the t/d contribution to d/b still neglected. But t/d can be estimated by using eqns (46) and (48) in the relation

$$\frac{P}{EL^2} = 8\frac{\sigma}{E}\left(\frac{b}{L}\right)^2\left(\frac{d}{b}\right)\left(\frac{t}{d}\right) \tag{49}$$

obtained from (43) and this gives simply

$$\frac{t}{d} = \frac{3}{4}\left(\frac{\rho_c}{\rho}\right)\left(1-\frac{1}{2}\frac{\rho_c}{\rho}\right)^{-1} \tag{50}$$

for all values of the structural index in the elastic design range. Note that for $\rho_c/\rho = 0.1$, $t/d \approx 0.079$, which justifies neglecting $\frac{1}{3}(t/d)^2$ relative to unity in eqn (41).

This simplification will no longer be made in the calculation that follows for values of the

structural index higher than the critical value $[P/(EL^2)]_Y$ for which σ_{opt} becomes equal to σ_Y. From eqn (46) we have

$$\left[\frac{P}{EL^2}\right]_Y = \frac{36\sqrt{1-\nu^2}}{\pi^3}\frac{\rho_c/\rho}{1-\frac{1}{2}\rho_c/\rho}\varepsilon_Y^{5/2} \tag{51}$$

and for all larger values of the structural index we can set $\sigma = \sigma_Y$ in eqn (44) and write

$$\frac{W}{\rho L^3} = \frac{[1-\frac{1}{2}\rho_c/\rho][P/(EL^2)]}{\varepsilon_Y} + \frac{4\rho_c}{\rho}\left(\frac{b}{L}\right)^2\frac{d}{b}. \tag{52}$$

To minimize W and also avoid column buckling, the optimum choice in (48) for b/L, with $\sigma_{opt}/E = \varepsilon_Y$ is dictated, giving

$$\frac{W}{\rho L^3} = \frac{[1-\frac{1}{2}\rho_c/\rho][P/(EL^2)]}{\varepsilon_Y} + \frac{24}{\pi^2}\frac{\rho_c}{\rho}\frac{d}{b}\varepsilon_Y. \tag{53}$$

Similarly, the best choice for d/b, following (4), should satisfy

$$\left(\frac{d}{b}\right)^2 = \left(\frac{1-\nu^2}{\pi^2}\right)\varepsilon_Y - \frac{1}{3}\left(\frac{t}{b}\right)^2 \tag{54}$$

and using (49) and (48) to eliminate t/b gives

$$\frac{d}{b} = \sqrt{\frac{1-\nu^2}{\pi^2}\varepsilon_Y - \frac{1}{3}\left[\frac{\pi^2 P/(EL^2)}{48\varepsilon_Y^2}\right]^2}. \tag{55}$$

With this optimum value of d/b, eqn (53) provides W_{min} and its use in (49) also gives the optimum dimension ratio

$$\frac{t}{d} = \frac{\sqrt{\dfrac{\pi^2 P}{48EL^2}}}{\varepsilon_Y^2(d/b)}. \tag{56}$$

These results are only valid up to the limiting value of the structural index that gives $t/d = 1$, for which there is no longer any filler in the sandwich walls. This limiting value is precisely that given earlier in eqn (30) for the transition to plasticity of the solid-wall hollow-core column; for higher values of the structural index, the squashing optimum weight is attained.

With the usual substitution of P/λ for P, the minimum-weight results for the sandwich-wall square-tube column are shown in Fig. 13, together with the curves of Fig. 11. The sandwich-wall square is more efficient than the hollow square, at least up to $[P/(\lambda EL^2)]_S = 5.18\times10^{-6}$, where optimum sizing demands that no sandwich filler at all be used and it coincides with the squashing solid-wall hollow tube. But for lower values of the structural index, the hollow circle still weighs less. The optimizing dimension ratios of the sandwich-wall square tube (see Fig. 12) are shown in Fig. 14. Yield starts at $[P/(\lambda EL^2)]_Y = 0.47\times10^{-6}$, but foam is still present up to $[P/(\lambda EL^2)]_S$, where $t/d = 1$. Then the foam disappears and as for the hollow, solid-wall tube, the values of b/L and d/b

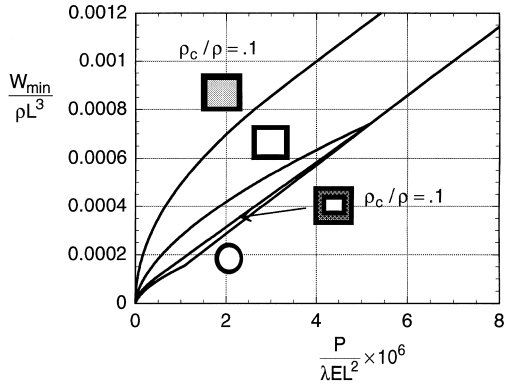

Fig. 13. Minimum column weights: foam-core square, hollow square, sandwich-wall square, hollow circle; $\varepsilon_Y = 0.007$, $v = 1/3$.

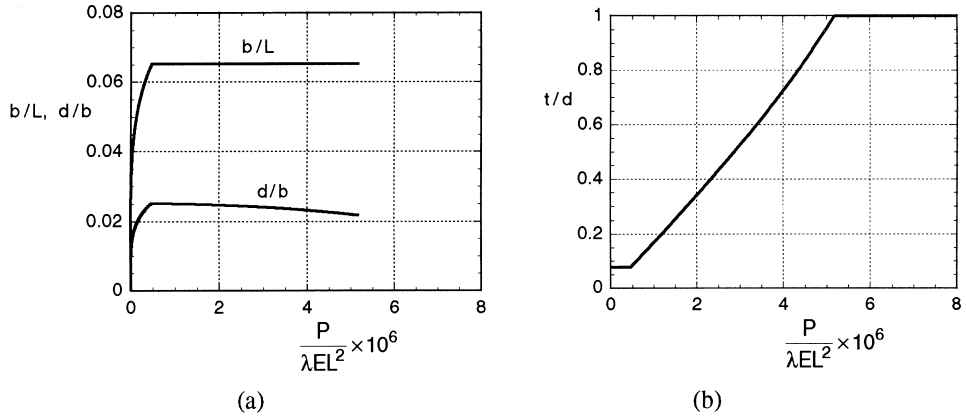

Fig. 14. Optimizing dimension ratios (Fig. 12) for sandwich-wall square tube; $\rho_c/\rho = 0.01$, $\varepsilon_Y = 0.007$, $v = 1/3$.

become indeterminate, subject only to the previously discussed constraints (31), (32), with t replaced by $2d$.

A passing remark: in the initial elastic range of structural index below $[P/(\lambda EL^2)]_Y$, the ratio of core weight to sheet weight is close to

$$\frac{W_c}{W_s} = \frac{2}{3}\left(1 - \frac{5}{4}\frac{\rho_c}{\rho}\right). \tag{57}$$

2.8. Hollow sandwich-wall circular cylinders

To round out the column efficiency studies, the sandwich-wall, hollow circular cylinder illustrated in Fig. 15 will be analyzed, although it has to be noted from Fig. 13 that there remains little room for improvement.

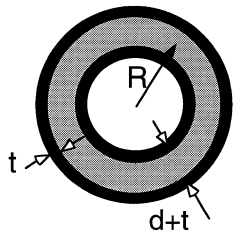

Fig. 15. Sandwich-wall, hollow cylinder; d = distance between sheet centerlines, t = sheet thickness, R = mean cylinder radius.

For small d/R, the column buckling stress σ_1 is still well approximated by eqn (33). For long tubes the local buckling stress of the sandwich cylinder may be written as (Anon., 1965)

$$\sigma_2 = \frac{2\gamma E}{\sqrt{1-\nu^2}}\frac{r_g}{R} \tag{58}$$

where r_g is the radius of gyration of the stress-carrying area of the shell and γ is the knockdown factor. We follow the NASA suggestion (Anon., 1967) and use eqn (35) for γ, where now

$$\phi = \frac{1}{16(12)^{1/4}}\sqrt{\frac{R}{r_g}}. \tag{59}$$

(Note that this reduces to the definition (36) for the solid hollow cylinder of Fig. 3.) For the sandwich cylinder

$$\frac{r_g}{R} = \frac{d}{2R}\sqrt{1+\frac{1}{3}\left(\frac{t}{d}\right)^2}. \tag{60}$$

Now follow the procedures used for the sandwich-wall square tube. Setting $\sigma_1 = \sigma_2 = \sigma$, provides the connections

$$\frac{\sigma}{E} = \frac{\pi^2}{2}\left(\frac{R}{L}\right)^2 = \frac{\gamma}{\sqrt{1-\nu^2}}\frac{d}{R}\sqrt{1+\frac{1}{3}\left(\frac{t}{d}\right)^2}. \tag{61}$$

The exact relations

$$P = 4\pi\sigma Rt \tag{62}$$

and

$$W = [4\pi\rho Rt + 2\pi\rho_c R(d-t)]L \tag{63}$$

give

$$\frac{W}{\rho L^3} = \frac{\left(1-\frac{1}{2}\frac{\rho_c}{\rho}\right)\frac{P}{EL^2}}{\sigma/E} + \frac{2\pi\rho_c}{\rho}\left(\frac{R}{L}\right)^2\frac{d}{R}. \tag{64}$$

For the elastic design range, we anticipate that t/d may be dropped in (61) and rewrite eqn (64) as

$$\frac{W}{\rho L^3} = \frac{\left(1-\frac{1}{2}\frac{\rho_c}{\rho}\right)\frac{P}{EL^2}\sqrt{1-\nu^2}}{(d/R)\gamma} + \frac{4\rho_c}{\pi\rho}\frac{\gamma}{\sqrt{1-\nu^2}}\left(\frac{d}{R}\right)^2. \tag{65}$$

In the definition (35) of γ, ϕ can be approximated by

$$\phi = \frac{1}{16(3)^{1/4}\sqrt{d/R}}. \tag{66}$$

Asserting that the derivative of $W/(\rho L^3)$ with respect to d/R must vanish leads to an explicit analytic formula for $P/(EL^2)$ in terms of the corresponding optimum d/R, which may then be used in eqn (65) to give the associated value of $W_{\min}/(\rho L^3)$; details are omitted. These elastic results are valid up to the critical value $[P/(EL^2)]_Y = 0.1323\times10^{-6}$ of the structural index, for which $\sigma/E = \varepsilon_Y(\gamma d/R)/\sqrt{1-\nu^2}$. At this point, for $\varepsilon_Y = 0.007$ and $\nu = 1/3$, the knockdown factor becomes equal to $\gamma_Y = 0.6595$, with $d/R = 0.0100$.

Note that for higher values of $P/(EL^2)$, eqns (58), (59), with $\sigma_2 = \sigma_Y$, imply that γ stays fixed at the value γ_Y. Using $\sigma = \sigma_Y$ in eqns (62) and (61) (with all terms now retained) to eliminate R/L and t/d from (64), gives

$$\frac{W_{\min}}{\rho L^3} = \frac{\left(1-\frac{1}{2}\frac{\rho_c}{\rho}\right)\frac{P}{EL^2}}{\varepsilon_Y} + \frac{4\rho_c}{\pi\rho}\frac{d}{R}\varepsilon_Y \tag{67}$$

in the range $[P/(EL^2)]_Y \leqslant P/(EL^2) \leqslant [P/(EL^2)]_s$, with

$$\frac{d}{R} = \sqrt{\frac{(1-\nu^2)\varepsilon_Y^2}{\gamma_Y^2} - \frac{1}{3}\left[\frac{\pi P/(EL^2)}{8\varepsilon_Y^2}\right]^2}. \tag{68}$$

The squash value $[P/(EL^2)]_s = 1.08\times10^{-6}$, corresponding to $t/d = 1$ and disappearance of the sandwich core, is the same as that found earlier for the monocoque cylinder. The other optimum dimension ratios in this range are

$$\frac{R}{L} = \frac{\sqrt{2\varepsilon_Y}}{\pi}, \quad \frac{t}{d} = \frac{\pi}{8\varepsilon_Y^2}\left(\frac{d}{R}\right)^{-1}\left(\frac{P}{EL^2}\right). \tag{69}$$

With the insertion of the mode-coupling λ into the structural index, the results for minimum weight

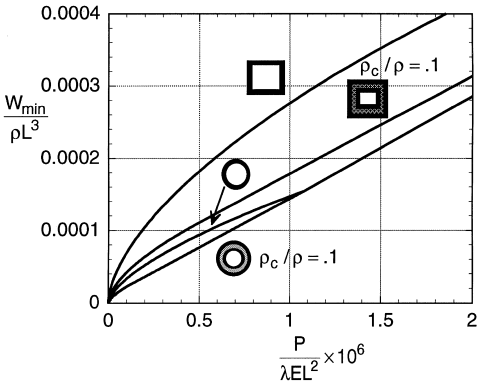

Fig. 16. Minimum weights of sandwich-wall, hollow circular cylinder and of other configurations; $\varepsilon_Y = 0.007$, $\nu = 1/3$.

of the sandwich-wall circular tube are shown by the bottom curve in Fig. 16, which zooms onto the design range for which sandwich tues provide lower weights than monocoque cylinders. Such low values of structural index correspond to long or lightly loaded columns, but unless L is unusually big, the core and sheet thicknesses required to optimize the design may be impractically small. Example: say $L = 14$ ft, $E = 10^7$ psi, $P = 50$ kips and $\lambda = 0.9$. Then $P/(\lambda EL^2) \approx 0.20 \times 10^{-6}$ and from eqns (68), (69), $R \approx 6.4''$, $t \approx 0.011''$ and the core thickness is $(d-t) \approx 0.053''$. This last dimension is less than the average cell size in currently available metal foams. A similar observation applies to the optimum dimensions of the sandwich-wall square tube.

3. Strain hardening

The optimization calculations can also be done on the basis of a strain-hardening stress–strain relation for the base material (Gerard, 1956). This has the conceptual advantage of permitting a unified calculation of plastic buckling that replaces the separate analyses for elastic and plastic behavior that were needed for ideal plasticity. The procedure will now be exemplified for the case of the hollow square tube.

The Ramberg–Osgood equation

$$\frac{\varepsilon}{\varepsilon_Y} = \frac{\sigma}{\sigma_Y} + \frac{3}{7}\left(\frac{\sigma}{\sigma_Y}\right)^n \tag{70}$$

connecting compressive stress σ and compressive strain ε will be used. Here σ_Y is a nominal yield stress, $\varepsilon_Y = \sigma_Y/E$ and $n > 1$ is the strain-hardening exponent. The plastic column buckling stress σ_1 of the hollow square-tube column (Fig. 3) is given by the Shanley (1946, 1947) result

$$\sigma_1 = \frac{\pi^2 E_{\tan}}{6}\left(\frac{b}{L}\right)^2 \tag{71}$$

for small t/b, where the tangent-modulus $E_{\tan}$, replacing E in eqn (1), depends on σ_1. The plate buckling stress will be written as

$$\sigma_2 = \frac{\pi^2 E_p}{3(1-\nu_p^2)}\left(\frac{t}{b}\right)^2 \tag{72}$$

where E_p and ν_p, replacing E in eqn (25), are functions of σ_2. The choices to be made here for E_p and ν_p are given by the modified deformation-theory formulas[2] (Stowell and Pride, 1951)

$$\eta_p \equiv \frac{E_p}{E} = \frac{E_{sec}}{E}\left[\frac{1}{2} + \frac{1}{4}\sqrt{1+\frac{3E_{\tan}}{E_{sec}}}\right] \tag{73}$$

$$\nu_p = \frac{1}{2} - \left(\frac{1}{2} - \nu\right)\frac{E_{sec}}{E} \tag{74}$$

in terms of the secant modulus E_{sec}. For the Ramberg–Osgood representation (70) we have

$$\eta_t \equiv \frac{E_{\tan}}{E} = \left[1 + \frac{3n}{7}\left(\frac{\sigma}{\sigma_Y}\right)^{n-1}\right]^{-1} \tag{75}$$

and

$$\eta_s \equiv \frac{E_{sec}}{E} = \left[1 + \frac{3}{7}\left(\frac{\sigma}{\sigma_Y}\right)^{n-1}\right]^{-1} \tag{76}$$

as functions of the applied stress.

Now impose the condition $\sigma_1 = \sigma_2 = \sigma_0$, where σ_0 is the naive optimization stress corresponding to the prescribed load P/λ. Then the optimum dimension ratios are

$$\frac{b}{L} = \frac{1}{\pi}\sqrt{\frac{6\varepsilon_Y}{\eta_t}\frac{\sigma_0}{\sigma_Y}} \tag{77}$$

and

$$\frac{t}{b} = \frac{1}{\pi}\sqrt{\frac{3(1-\nu_p^2)\varepsilon_Y}{\eta_p}\frac{\sigma_0}{\sigma_Y}}. \tag{78}$$

Using $P = 4bt\sigma_0$ and $W = \rho PL/\sigma_0$ then gives

[2] A spirited debate raged 50 years ago about the 'right' equations for plastic buckling of plates and shells and has been renewed occasionally since then. Suffice it to say here that the deformation-theory results shown here have withstood the test of time, even if one prefers to regard them as semi-empirical.

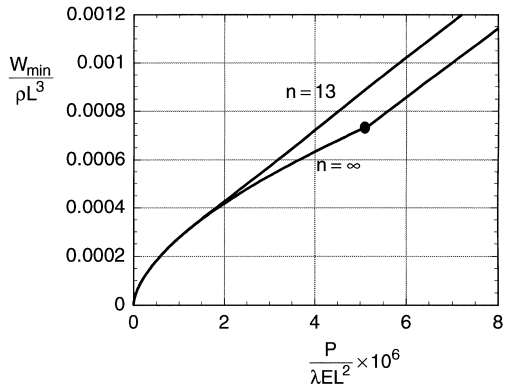

Fig. 17. Minimum weight of hollow square tube for strain-hardening ($n = 13$) and ideal plasticity ($n = \infty$); $\varepsilon_Y = 0.007$, $\nu = 1/3$.

$$\frac{P}{EL^2} = 4\varepsilon_Y \left(\frac{b}{L}\right)^2 \left(\frac{t}{L}\right)\left(\frac{\sigma_0}{\sigma_Y}\right) \tag{79}$$

and

$$\frac{W_{\min}}{\rho L^3} = \frac{1}{\varepsilon_Y}\left(\frac{P}{EL^2}\right)\left(\frac{\sigma_0}{\sigma_Y}\right)^{-1}. \tag{80}$$

For prescribed values of ε_Y and n, eqns (73)–(80) provide $W_{\min}/(\rho L^3)$, as well as b/L and t/b, as functions of $P/(EL^2)$, parametrically via σ_0/σ_Y. (These results with strain hardening taken into account were essentially given by Gerard (1956), except that he used $\eta_p = \eta_s$.)

With the mode-interaction factor λ introduced into the denominator of the abscissa, the minimum-weight results are shown in Fig. 17 for $n = 13$ and $\varepsilon_Y = 0.007$, together with the curve of Fig. 8 for $n = \infty$. (Note that in the strain-hardening Ramberg–Osgood formulation plastic deformation occurs for $\sigma/\sigma_Y < 1$, which is why the weights are higher for $n = 13$ than for $n = \infty$.) The optimum dimension ratios are shown in Fig. 18. These may be compared with the results of Fig. 8 for $n = \infty$. Note that with plastic buckling as the failure criterion in the presence of strain-hardening, the optimum dimensions are determinate at all values of the structural index.

Similar procedures can be used to account for strain hardening in the optimization of the other configurations that have been studied via ideal plasticity. Suffice it to say that strain hardening is not likely to change the qualitative conclusions reached concerning the relative weights of various optimum designs.

4. Panels

Wide panels stiffened by uniformly spaced longitudinal stringers (Fig. 19) are common compression components in aircraft structures. The minimum weight design of such panels received much attention 50 years ago, in a remarkable series of systematic compressive strength tests of

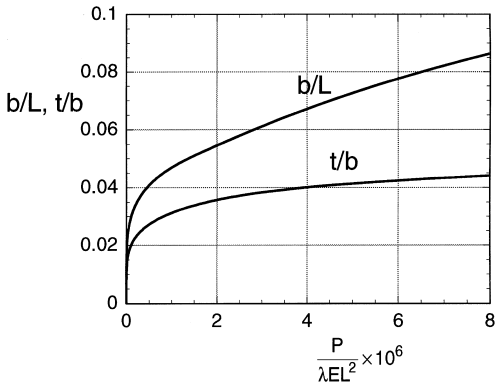

Fig. 18. Optimum dimension ratios, hollow square tube; $n = 13$, $\varepsilon_Y = 0.007$, $\nu = 1/3$.

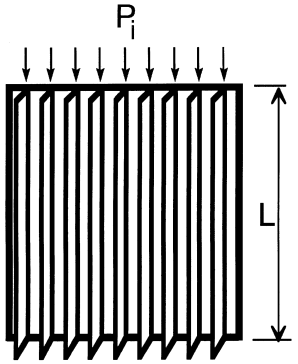

Fig. 19. Stiffened compression panel: P_i = load per unit width.

hundreds of panels by the National Advisory Committee for Aeronautics (NACA), e.g., Schuette (1945), Schuette et al. (1946), Hickman and Dow (1951, 1953) and more. In addition, a few theoretical papers were written by engineers at Lockheed (Zahorski, 1944), Bristol Aeroplane (Farrar, 1949) and Vickers-Armstrong (Catchpole, 1954). The panel is essentially a wide column and if simple support is assumed, the elastic Euler column buckling stress is

$$\sigma_1 = \frac{\pi^2}{A_i}\frac{EI_i}{L^2} \tag{81}$$

where A_i is the average cross-sectional area per unit width and I_i is the centroidal moment of inertia per unit width. The stress σ produced by a load per unit width P_i is $\sigma = P_i/A_i$ and it follows that σ_1 and the corresponding P_i when column buckling occurs are related by

$$\sigma_1 = (\pi^2 E\omega)^{1/3}\left(\frac{P_i}{L}\right)^{2/3} \tag{82}$$

where $\omega = I_i/A_i^3$ is the panel shape factor (Schuette, 1945). This displays the fundamental panel

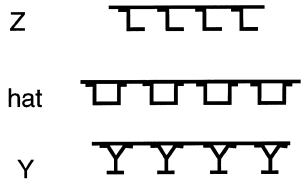

Fig. 20. Z, hat and Y stiffeners.

structural index P_i/L containing the prescribed design variables. Maximizing σ_1 minimizes the weight per unit length $W_i = \rho P_i L/\sigma_1$. Thus, for a given material, the optimum design problem devolves upon a search for the highest admissible ω, at least in the elastic design range.

Figure 19 illustrate so-called 'blade' stiffeners; the NACA tests involved riveted Z, hat and Y stringers (Fig. 20), the first two of which have been most commonly used in practice. In all cases, local buckling provides an upper bound to ω and naive optimization demands the equality of local and column buckling. This has general implications concerning the dependence of minimum weight on the structural index (Zahorski, 1944). For any one of the stiffener configurations shown in Figs (19–20), the elastic local buckling stress σ_2 will obey the functional form

$$\frac{\sigma_2}{E} = f_2 \left(\frac{t}{b}\right)^2 \tag{83}$$

where b is the stiffener spacing, t is the skin thickness and the nondimensional coefficient f_2 depends only on the remaining independent ratios of pertinent dimensions within the repeating unit of the skin-stiffener combination. For these ratios fixed, the shape factor $\omega = I_i/A_i^3$ will generally be proportional to $(b/t)^2$ and so the column buckling stress in (82) satisfies

$$\frac{\sigma_1}{E} = f_1 \left(\frac{b}{t}\right)^{2/3} \left(\frac{P_i}{EL}\right)^{2/3} \tag{84}$$

where f_1 is another coefficient dependent on dimension ratios. Accordingly, with the imposition of the naive optimization condition $\sigma = \sigma_1 = \sigma_2$, elimination of t/b gives

$$\frac{\sigma}{E} = (f_1^3 f_2)^{1/4} \sqrt{\frac{P_i}{EL}}. \tag{85}$$

A further search for the proportions that provide the optimum value $\alpha \equiv [(f_1^3 f_2)^{1/4}]_{\max}$ would give

$$\frac{\sigma_{\text{opt}}}{E} = \alpha \sqrt{\frac{P_i}{EL}} \tag{86}$$

and then the minimum weight per unit width W_i is $\rho P_i L/\sigma_{\text{opt}}$.

The NACA tests, in effect, solved the problem of finding σ_{opt} experimentally. They actually went much further, exploring the plasticity range for the connection between α and P_i/L as well, for two aluminum alloys. The tests also inherently took into account many practical variables such as the

Table 1
Value of α, eqn (86)

	NACA	Farrar
Z	1.02	0.95
Hat	0.99	0.96
Y	1.15	1.25

real details of riveted connections and rivet spacing and other actual as opposed to idealized cross-sectional geometries.

The NACA experimental results for σ_{opt} in the elastic range were summarized by Gerard (1956) as shown in Table 1, which gives the value of α in eqn (86) that he extracted from the voluminous NACA data for Z, hat and Y stiffeners. Farrar (1949), working independently, analyzed the optimization problem theoretically, producing the results for α shown for comparison in Table 1. The agreement is remarkable. Later, Catchpole (1954) analyzed the blade-stiffened panel and found $\alpha = 0.81$.

To establish a simple baseline result for near-optimum skin-stringer panels that can easily be extended to the plastic design range, the special hat-stiffened configuration shown in Fig. 21 is considered. The construction is idealized to be integral, without attachment flanges, skin and stringer thicknesses t are equal and the identical, centerline stringer flange and web lengths b are half the stringer pitch $2b$. The local plastic buckling stress σ_2 is then exactly the same as for a square tube and so is given by eqn (72), with the plasticity definitions (73)–(76) applicable. The plastic column buckling stress σ_1 is given by eqn (82), with E replaced by the tangent modulus E_t and with $\omega = (52/1875)(b/t)^2$, which follows from $I_i = (13/30)b^2t$ and $A_i = 5t/2$. Setting $\sigma_0 = \sigma_1 = \sigma_2$ and eliminating b/t, as in the general derivation of eqn (85), gives the naive-optimum stress

$$\frac{\sigma_0}{\sigma_Y} = \frac{\pi}{5\varepsilon_Y}\left(\frac{2}{3}\right)^{1/2}\left(\frac{13\eta_t\eta_p}{1-\nu_p^2}\right)^{1/4}\left(\frac{P_i}{EL}\right)^{1/2} \tag{87}$$

where η_t, η_p and ν_p are functions of σ_0/σ_Y. This result, in essence, was found by Zahorski (1944); here the new nondimensional structural index $P_i/(EL)$ has been introduced. In the elastic range, with $\nu = 1/3$ and $\eta_t = \eta_p = 1$, eqn (87) provides the approximation $\alpha \approx 1.00$ in eqn (86), close to

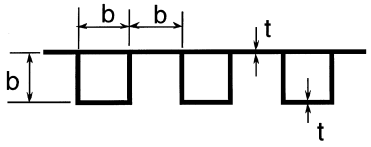

Fig. 21. Special hat-stiffened panel.

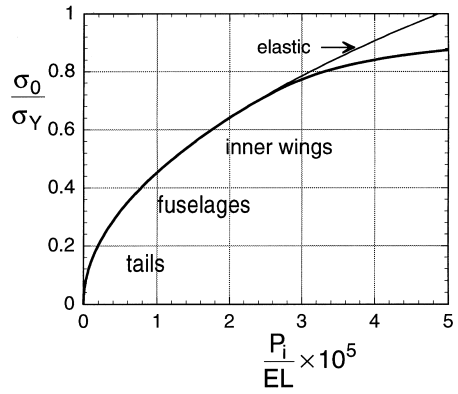

Fig. 22. Stress in naive-optimum, stiffened panel (Fig. 21); $n = 21$, $\varepsilon_Y = 0.007$, $\nu = 1/3$.

the optimum result in the NACA tests. Figure 22 shows the graph of eqn (87) for $n = 21$ and $\varepsilon_Y = 0.007$, together with the elastic result. The rough ranges of structural index indicated for panels in various aircraft components are adapted from Farrar's 1949 paper. The naive-optimum nondimensional weight is

$$\left(\frac{W_i}{\rho L^2}\right)_{\min} = \frac{P_i}{\varepsilon_Y EL} \Big/ \frac{\sigma_0}{\sigma_Y}. \tag{88}$$

In terms of σ_0/σ_Y, t/b is given by eqn (78) and from eqn (81), with E replaced by E_t, we have

$$\frac{b}{L} = \frac{1}{\pi}\sqrt{\frac{(75/13)(\sigma_0/\sigma_Y)\varepsilon_Y}{\eta_t}}. \tag{89}$$

Finally, P_i may be replace by P_i/λ in these results to account for mode interaction. Curves showing weight and dimension ratios vs $P_i/(\lambda EL)$, found parametrically via σ_0/σ_Y, are given in Figs 23 and 24 for $n = 21$ and $\varepsilon_Y = 0.007$. At least in the elastic range, λ should probably not be less than 0.9

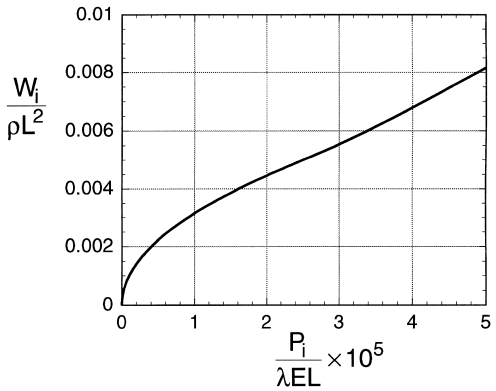

Fig. 23. Weight of hat-stiffened panel (Fig. 21); $n = 21$, $\varepsilon_Y = 0.007$, $\nu = 1/3$.

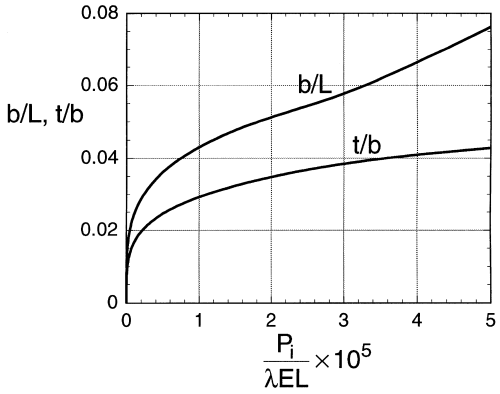

Fig. 24. Optimum dimension ratios of hat-stiffened panel (Fig. 21); $n = 21$, $\varepsilon_Y = 0.007$, $\nu = 1/3$.

(Koiter and Pignataro, 1976). The result (88) for the minimum weight can be written more explicitly as

$$\frac{W_i}{\rho L^2} = \frac{5}{\pi}\left(\frac{3}{2}\right)^{1/2}\left(\frac{1-\nu_p^2}{13\eta_t\eta_p}\right)^{1/4}\left(\frac{P_i}{\lambda EL}\right)^{1/2} \tag{90}$$

which shows that in the elastic range it varies like the square root of the structural index.

A symmetrical foam-core sandwich panel (Fig. 25) is examined next. The weight per unit width is $W_i = [2\rho t + \rho_c(d-t)]L$ and using $2t = P_i/\sigma$ gives

$$\frac{W_i}{\rho L^2} = \frac{\dfrac{P_i}{EL}\left(1-\dfrac{\rho_c}{2\rho}\right)}{\varepsilon_Y\sigma/\sigma_Y} + \frac{\rho_c}{\rho}\frac{d}{L}. \tag{91}$$

Here σ is the column buckling stress satisfying

$$\frac{\sigma}{\sigma_Y} = \frac{\pi^2}{4}\frac{\eta_t}{\varepsilon_Y}\left(\frac{d}{L}\right)^2 \tag{92}$$

for $(t/d)^2 \ll 1$. (In the pertinent range of structural index, it will not be necessary to account for thicker skins.) Eliminating d/L from eqn (91) gives

Fig. 25. Sandwich panel; d = distance between centerlines of face-sheets.

$$\frac{W_i}{\rho L^2} = \frac{\dfrac{P_i}{EL}\left(1-\dfrac{\rho_c}{2\rho}\right)}{\varepsilon_Y \sigma/\sigma_Y} + \frac{2\rho_c}{\pi\rho}\sqrt{\frac{\varepsilon_Y}{\eta_t}}\sqrt{\frac{\sigma}{\sigma_Y}} \tag{93}$$

and with the use of eqn (75) for η_t this may be minimized with respect to σ/σ_Y, with the result

$$\frac{P_i}{EL}\left(1-\frac{\rho_c}{2\rho}\right) = \frac{\rho_c}{\pi\rho}\left(\frac{\varepsilon_Y \sigma}{\sigma_Y}\right)^{3/2} \frac{n-(n-1)\eta_t}{\sqrt{\eta_t}}. \tag{94}$$

The optimum d/L, the minimum weight and the corresponding value of the structural index are now explicit in terms of σ/σ_Y via eqns (92)–(94) and then the optimum t/d is given by

$$\frac{t}{d} = \frac{\dfrac{P_i}{EL}}{2\varepsilon_Y(\sigma/\sigma_Y)(d/L)}. \tag{95}$$

Plots of the minimum weight are shown in Fig. 26 for $\rho_c/\rho = 0.05$ and 0.1, together with the results of Fig. 23 for comparison. Figure 27 shows the optimum dimension ratios for $\rho_c/\rho = 0.1$.

The elastic solution for minimum sandwich weight per unit width is

$$\frac{W_i}{\rho L^2} = \frac{3}{\pi^{2/3}}\left(\frac{\rho_c}{\rho}\right)^{2/3}\left(1-\frac{\rho_c}{2\rho}\right)^{1/3}\left(\frac{P_i}{EL}\right)^{1/3} \tag{96}$$

which shows that as a function of the structural index the optimized sandwich must always start out weighing more than the optimized stiffened panel [eqn (90)]. Furthermore, in the examples shown, plasticity prevents the sandwich weight from ever getting smaller than that of the skin-stringer panel, which it would inevitably do in an ideal elastic world.

In the elastic solution, the optimum skin thickness is given by

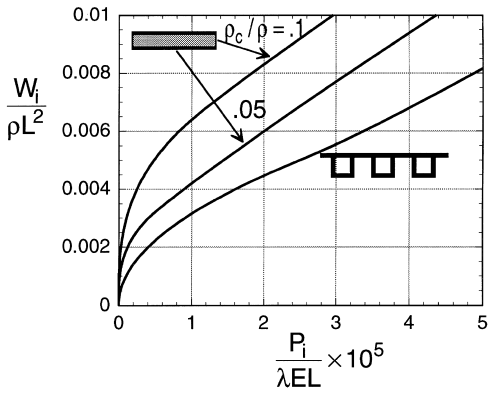

Fig. 26. Minimum weights, sandwiches vs stiffened panel; $n = 21$, $\varepsilon_Y = 0.007$, $v = 1/3$.

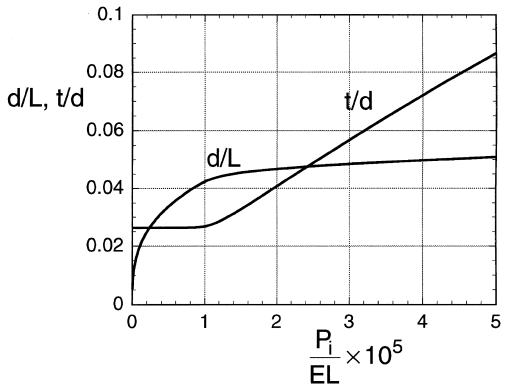

Fig. 27. Optimum dimension ratios of sandwich panel; $\rho_c/\rho = 0.01$, $n = 21$, $\varepsilon_Y = 0.007$.

$$\frac{t}{d} = \frac{\rho_c}{4\rho}\left(1 - \frac{\rho_c}{2\rho}\right)^{-1} \tag{97}$$

and the corresponding ratio of core weight to skin weight is

$$\frac{W_c}{W_s} = 2\left(1 - \frac{3\rho_c}{4\rho}\right). \tag{98}$$

(This provides a first-order correction to the well-known condition $W_c/W_s = 2$ for minimizing the weight of a sandwich with a very light core when its bending stiffness is prescribed.)

Finally, the idealized panel configuration illustrated in Fig. 28, where the stringer pitch is fixed at $2b$, will be optimized; here both the skin and stringer walls are sandwiches. Equating the column and local buckling stresses gives the naive optimization condition

$$\sigma = \frac{13\pi^2 E_{\tan}}{75}\left(\frac{b}{L}\right)^2 = \frac{\pi^2 E_p}{(1-\nu_p^2)}\left(\frac{d}{b}\right)^2\left[1 + \frac{1}{3}\left(\frac{t}{d}\right)^2\right] = \frac{P_i/L}{5\left(\frac{b}{L}\right)\left(\frac{d}{b}\right)\left(\frac{t}{d}\right)} \tag{99}$$

and the weight per unit width is

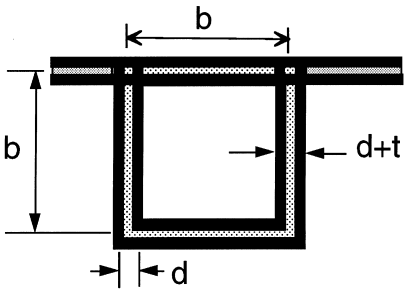

Fig. 28. Sandwich-wall skin and stringer; t = face-sheet thicknesses, b = centerline widths, d = distance between face-sheet centerlines.

$$W_i = [5\rho t + (5\rho_c/2)(d-t)]L. \tag{100}$$

These can be manipulated to produce the expression

$$\frac{W_i}{\rho L^2} = \frac{\dfrac{P_i}{EL}\left(1-\dfrac{\rho_c}{2\rho}\right)}{\varepsilon_Y \sigma/\sigma_Y} + \frac{5\rho_c}{2\rho}\left(\frac{d}{L}\right) \tag{101}$$

where

$$\frac{d}{L} = \sqrt{\frac{75}{13\pi^4}\frac{1-\nu_p^2}{\eta_t\eta_p}\left(\frac{\varepsilon_Y\sigma}{\sigma_Y}\right)^2 - \frac{1}{75}\left(\frac{P_i}{EL}\right)^2\left(\frac{\varepsilon_Y\sigma}{\sigma_Y}\right)^{-2}}. \tag{102}$$

To establish minimum weight for a given value of the structural index, the derivative of (101) with respect to σ/σ_Y is set to equal to zero; here, numerical differentiation, based on the definitions (74)–(76) is convenient. The resulting equation may readily be solved iteratively for $P_I/(EL)$ vs assumed values of σ/σ_Y and then the relations (101) and (102), together with

$$\frac{b}{L} = \frac{1}{\pi}\sqrt{\frac{75}{13}\frac{\varepsilon_Y}{\eta_t}\frac{\sigma}{\sigma_Y}} \tag{103}$$

and

$$\frac{t}{d} = \frac{\dfrac{P_i}{EL}}{5\varepsilon_Y(\sigma/\sigma_Y)(d/L)} \tag{104}$$

provide the results shown by the bottom curve in Fig. 29 for minimum weight and in Fig. 30 for optimum dimension ratios. Using $\lambda = 0.9$ here should be conservative.

Although the optimum sandwich-wall skin-stringer panel clearly provides the lowest weight in

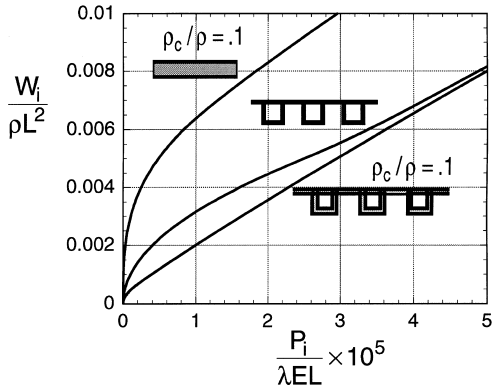

Fig. 29. Optimum weights: sandwich panel, hat-stiffened panel, sandwich skin and stringer panel; $n = 21$, $\varepsilon_Y = 0.007$, $\nu = 1/3$.

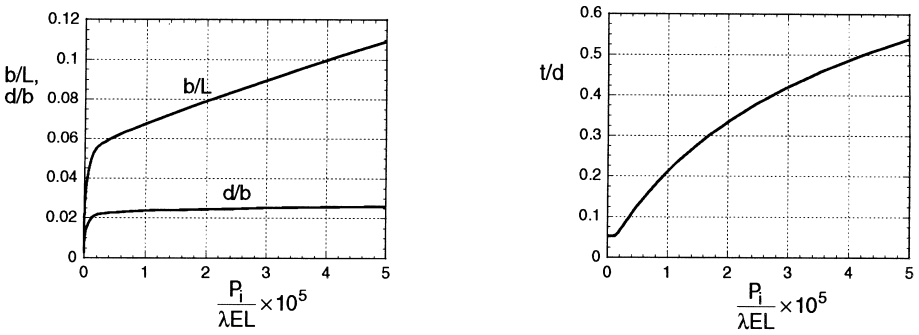

Fig. 30. Optimum dimension ratios of sandwich-wall skin-stringer panel (Fig. 28); $\rho_c/\rho = 0.01$, $n = 21$, $\varepsilon_Y = 0.007$, $\nu = 1/3$.

the low range of the structural index, the practicality of the required dimensions is questionable. As in a sandwich-wall column, the optimum core thickness may become of the order of the cell size in a metal foam.

In the small range of structural index, say $P_i/(EL) \times 10^5 < 1/10$, where the design is essentially elastic,

$$t/d = (\rho_c/\rho)(2-\rho_c/\rho)^{-1} \tag{105}$$

and it follows that the ratio of core weight to sheet weight is

$$W_c/W_s = 1-\rho_c/\rho. \tag{106}$$

But as the structural index increases, t/d approaches unity and the optimum core thickness $(d-t)$ tends to zero.

5. Concluding remarks

The present optimization studies were made in order to assess the potential utility of light metal foams as weight-saving components of two kinds of compression structures: columns and flat compression panels. For foam porosities around 90%, the results are disappointing in some respects. On a weight/strength basis, foam-core square and circular tubes appear to be generally inferior to optimized, hollow columns; optimized flat sandwich compression panels are heavier than optimized skin-stringer panels. In principle, using sandwiches as the walls of hollow columns can provide weight savings and lower weight in a stiffened panel can be attained by substituting sandwiches for the monolithic walls of the skin and stringers. But in structures of conventional scales, such hypothetical designs tend to be impractical because of minimum-gage considerations with respect to core and face-sheet thicknesses.

There are several compelling reasons, however, why metal–foam sandwich construction should not be dismissed. These may be described succinctly as: cost, stiffness and multiple use. The first is obvious; economies of processing and fabrication could, in some applications, be more important considerations than weight. Stiffness: no limitations on axial compliance were imposed in the

present studies. Imposition of a stiffness requirement in addition to a specified axial strength tends to reduce the competition among various configurations. (This explains, at least partially, the results of the study by Cruz (1991), in which stiffness requirements, as well as limitations on axial strain, were indeed imposed and honeycomb-core sandwich panels turned out to be nearly as structurally efficient as skin-stringer panels.) With respect to multiple use, metal foam core sandwiches have already found applications in sound-insulating panels and show promise as fire retardants; these benefits could dominate weight considerations.

It should also be mentioned that purely on a weight basis, metal–foam sandwich construction may be very efficient in curved shells subjected to midsurface compression. The isotropic bending resistance in a sandwich having an isotropic core would appear to provide a structural advantage over stiffening in one direction when resistance to buckling is a design constraint. A limited number of numerical studies by Agarwal and Sobel (1972) have demonstrated weight advantages of optimized axially compressed sandwich cylinders over optimum designs of skin-stringer cylinders. Systematic, comparative optimization studies of curved shells are clearly desirable.

A few remarks follow about some of the idealizations made in the present sandwich analyses. Ignoring the in-plane core stiffness makes the sandwich appear a bit worse than it really is, but this conservative effect, for high-porosity foams, is small. On the other hand, the influence of transverse shear compliance in lower buckling resistance was also neglected and this could be more serious, especially for porosities that exceed 0.95. Core plasticity could also lower buckling resistance considerably. These may be good reasons to seek improvements in the stiffness and yield properties of metal foams, should their use as sandwich cores be contemplated. Finally, on the positive side, elementary estimates indicate that for porosities below 0.95, face-sheet wrinkling into metal–foam cores does not appear to be an issue, even with cores having relatively poor stiffness properties, as long as they remain elastic.

A final observation: the imperfection-sensitivity of optimized thin-walled columns and stiffened panels tends to make failures catastrophic when they occur, whereas foam-core columns and sandwich panels can be expected to undergo more graceful collapse. This qualitative consideration might nudge a prudent designer to accept the weight penalties associated with more robust configurations that exploit metal foams.

Acknowledgements

This work was partially supported by a DARPA University Research Initiative (Subagreement P.O. No. KK3007 with the University of California, Santa Barbara, ONR Prime Contract N00014-92-J-1808), a DARPA Multidisiplinary University Research Initiative (ONR Contract N00014-1-96-1028) and by the Division of Engineering and Applied Sciences, Harvard University.

References

Agarwal, B.L., Sobel, L.H., 1972. Weight comparisons of optimized stiffened, unstiffened and sandwich cylindrical shells. J. Aircraft 14 (10), 1000–1008.

Anon., 1965. Buckling of thin-walled circular cylinders. NASA Space Vehicle Design Criteria. NASA SP-8007.

Catchpole, E.J., 1954. The optimum design of compression structures having unflanged integral stiffeners. J. Royal Aeronautical Society 58, 765–768.
Cruz, J.R., 1991. Optimization of composite sandwich cover panels subjected to compressive loadings. NASA Technical Paper 3173.
Farrar, D.J., 1949. The design of compression structures for minimum weight. J. Royal Aeronautical Society 53, 1041–1052.
Gerard, G., 1956. Minimum Weight Analysis of Compression Structures. New York University Press, New York.
Hickman, W.A., Dow, N.F., 1951. Direct-reading design charts for 75S-T6 aluminum alloy flat compression panels having longitudinal extruded Z-section stiffeners. NACA Technical Note 2435.
Hickman, W.A., Dow, N.F., 1953. Direct-reading design charts for 24S-T3 aluminum alloy flat compression panels having longitudinal formed hat-section stiffeners and comparisons with panels having Z-section stiffeners. NACA Technical Note 2792.
Koiter, W.T., 1945. On the stability of elastic equilibrium (in Dutch). Thesis, Delft University, H.J. Paris, Amsterdam; English transl. (a) NASA TT-F10, 833, 1967, (b) AFFDL-70-25, 1970.
Koiter, W.T., Pignataro, M., 1976. A general theory for the interaction between local and overall buckling of stiffened panels. Report WTHD 83, Department of Mechanical Engineering, Delft University of Technology, The Netherlands.
Koiter, W., Skaloud, M., 1962. Comment in: Colloque sur le comportement postcritique des plaques utilisées en construction métallique. Mem. Soc. Roy. d. Sciènces de Liège 5 (8), 64–68, 103, 104.
Maquoi, R., Massonet, Ch., 1976. Interaction between local plate buckling and overall buckling in thin-walled compression members—theories and experiments. In: Budiansky, B. (Ed.), Proc. IUTAM Symposium on Buckling of Structures. Springer-Verlag pp. 365–382.
Schuette, E.H., 1945. Charts for the minimum weight design of 24S-T aluminum alloy flat compression panels with longitudinal Z-section stiffeners. NACA Technical Report 827.
Schuette, E.H., Barab, S., McCracken, H.L., 1946. Compressive strength of 24S-T aluminum alloy flat panels with longitudinal formed hat-section stiffeners. NACA Technical Note 1157.
Shanley, F.R., 1946. The column paradox. J. Aeronautical Sciences 13 (12), 678.
Shanley, F.R., 1947. Inelastic column theory. J. Aeronautical Sciences 14 (5), 261–267.
Shanley, F.R., 1952. Weight-Strength Analysis of Aircraft Structures. McGraw-Hill, New York.
Stowell, E.Z., Pride, R.A., 1951. The effect of compressibility of the material on plastic buckling stresses. Reader's Forum. J. Aeronautical Sciences 18 (11), 773.
Thompson, J.M.T., Lewis, G.M., 1972. On the optimum design of thin-walled compression members. J. Mech. Phys. Solids 20, 101–109.
Tvergaard, V., 1973. Imperfection-sensitivity of a wide integrally stiffened panel under compression. Int. J. Solids Structures 9, 177–192.
Wagner, H., 1929. Remarks on airplane struts and girders under compressive and bending stresses. Index values. NACA Technical Memorandum No. 500. (Translation of Einige Bemerkungen über Knickstabe und Biegungstrager. Der Kennwert., Zeitschrift fur Flugtechnik und Motorluftschiffahrt.) 14 June 1928, pp. 241–247.
Weaver, P.M., Ashby, M.F., 1997. An overview of material limits for shape efficiency. Engineering Department, Cambridge University, Cambridge, U.K.
Zahorski, A., 1944. Effects of material distribution on strength of panels. J. Aeronautical Sciences 11 (3), 247–253.